

# New Equations for the Sublimation Pressure and Melting Pressure of H<sub>2</sub>O Ice Ih

Wolfgang Wagner<sup>a)</sup> and Thomas Riethmann<sup>b)</sup>

*Lehrstuhl für Thermodynamik, Ruhr-Universität Bochum, D-44780 Bochum, Germany*

Rainer Feistel

*Leibniz-Institut für Ostseeforschung, Seestraße 15, D-18119 Warnemünde, Germany*

Allan H. Harvey

*Thermophysical Properties Division, National Institute of Standards and Technology,  
325 Broadway, Boulder, Colorado 80305, USA*

(Received 31 August 2011; accepted 14 October 2011; published online 5 December 2011)

New reference equations, adopted by the International Association for the Properties of Water and Steam (IAPWS), are presented for the sublimation pressure and melting pressure of ice Ih as a function of temperature. These equations are based on input values derived from the phase-equilibrium condition between the IAPWS-95 scientific standard for thermodynamic properties of fluid H<sub>2</sub>O and the equation of state of H<sub>2</sub>O ice Ih adopted by IAPWS in 2006, making them thermodynamically consistent with the bulk-phase properties. Compared to the previous IAPWS formulations, which were empirical fits to experimental data, the new equations have significantly less uncertainty. The sublimation-pressure equation covers the temperature range from 50 K to the vapor–liquid–solid triple point at 273.16 K. The ice Ih melting-pressure equation describes the entire melting curve from 273.16 K to the ice Ih–ice III–liquid triple point at 251.165 K. For completeness, we also give the IAPWS melting-pressure equation for ice III, which is slightly adjusted to agree with the ice Ih melting-pressure equation at the corresponding triple point, and the unchanged IAPWS melting-pressure equations for ice V, ice VI, and ice VII. [doi:10.1063/1.3657937]

Key words: ice Ih; ice III; ice V; ice VI; ice VII; melting-pressure equation; sublimation-pressure equation; water.

## CONTENTS

1. Introduction . . . . .	2	3.2. Range of validity and estimated uncertainty of the sublimation-pressure equation . . . . .	6
2. Input Data for the Development of the New Equations . . . . .	3	4. The New Melting-Pressure Equation for Ice Ih . . . . .	6
2.1. Input data for the sublimation-pressure equation . . . . .	3	4.1. Discussion, range of validity, and estimated uncertainty of the equation . . . . .	7
2.2. Input data for the melting-pressure equation for ice Ih . . . . .	4	5. Melting-Pressure Equations for Ice III, Ice V, Ice VI, and Ice VII . . . . .	7
3. The New Sublimation-Pressure Equation . . . . .	4	5.1. Melting-pressure equation for ice III . . . . .	7
3.1. Discussion of the sublimation-pressure equation . . . . .	5	5.2. Melting-pressure equations for ice V, ice VI, and ice VII . . . . .	8
		5.2.1. Range of validity and estimates of uncertainty of the equations . . . . .	8
		5.2.2. Computer-program verification . . . . .	8
		6. Acknowledgments . . . . .	8
		7. Appendix: Uncertainty Estimate for the Sublimation-Pressure Equation . . . . .	8
		8. References . . . . .	10

<sup>a)</sup>Author to whom correspondence should be addressed; Electronic mail: Wagner@thermo.rub.de.

<sup>b)</sup>Present address: STEAG Energy Services GmbH, Rüttenscheider Str. 1-3, D-45128 Essen, Germany.

### List of Tables

1.	Selected input data points on the sublimation curve calculated via the phase-equilibrium condition, Eq. (2), using the IAPWS-95 formulation for water vapor and the equation of state for ice Ih	3
2.	Selected input data points on the melting-pressure curve calculated via the phase-equilibrium condition, Eq. (3), using the IAPWS-95 formulation for liquid water and the equation of state for ice Ih	4
3.	Coefficients $a_i$ and exponents $b_i$ of the sublimation-pressure equation, Eq. (4)	4
4.	Coefficients $a_i$ and exponents $b_i$ of the melting-pressure equation, Eq. (6)	6
5.	Values for the triple points of the solid phases that coexist with another solid phase and with the liquid	8
6.	Estimated uncertainties of calculated melting pressures	8
7.	Melting pressures calculated from Eqs. (7) to (10) for selected temperatures	8

### List of Figures

1.	Phase-boundary curves of water in a $p$ - $T$ diagram	3
2.	Percentage deviations in sublimation pressure between the input data $p_{\text{subl,data}}$ and the values $p_{\text{subl,calc}}$ calculated with Eq. (4)	5
3.	Percentage deviations of experimental data for the sublimation pressure $p_{\text{subl,exp}}$ from values $p_{\text{subl,calc}}$ calculated with Eq. (4)	5
4.	Percentage deviations of experimental data for the sublimation pressure $p_{\text{subl,exp}}$ from values $p_{\text{subl,calc}}$ calculated with Eq. (4)	6
5.	Percentage uncertainties in sublimation pressure for the sublimation-pressure equation, Eq. (4), estimated with Eqs. (5a) and (5b)	6
6.	Percentage deviations in melting pressure between the input data $p_{\text{melt,data}}$ and the values $p_{\text{melt,calc}}$ calculated with Eq. (6)	7

### List of Symbols

$B$	= second virial coefficient
$c_p$	= isobaric heat capacity
$g$	= specific Gibbs energy
$p$	= pressure
$p_{\text{melt}}$	= melting pressure
$p_{\text{subl}}$	= sublimation pressure
$R$	= specific gas constant of water
$s$	= specific entropy
$T$	= absolute temperature; values correspond to the ITS-90 temperature scale

$U$	= expanded uncertainty ( $k=2$ )
$v$	= specific volume
$\delta$	= deviation of a quantity
$\pi$	= reduced pressure, $\pi = p_{\text{subl}}/p^*$ (Sec. 3) or $\pi = p_{\text{melt}}/p^*$ (Secs. 4 and 5)
$\theta$	= reduced temperature, $\theta = T/T^*$

### Superscripts

*	= reducing quantity
"	= property of water vapor at the sublimation-pressure curve
+	= property of ice Ih at the sublimation-pressure or melting-pressure curve
++	= property of liquid water at the melting-pressure curve
id	= property in the ideal-gas state
Ih	= property of ice Ih (solid phase "S" in Fig. 1)
vap	= property of water vapor (gas phase "G" in Fig. 1)

### Subscripts

o	= constant value
calc	= calculated value
data	= input data used to develop the equations
exp	= experimental value
t	= property at the several triple points; see Fig. 1

## 1. Introduction

Figure 1 shows the phase-boundary curves of water in a  $p$ - $T$  diagram. This article presents new equations for the calculation of pressures along the sublimation-pressure curve and the melting-pressure curve of ice Ih. These curves are plotted in bold in Fig. 1.

In 1993, IAPWS issued a "Release on the Pressure along the Melting and Sublimation Curves of Ordinary Water Substance;" the corresponding article was published in 1994.<sup>1</sup> These empirical equations were fitted to relatively old experimental data for the sublimation-pressure curve and for the several sections of the melting-pressure curve; see Fig. 1. Thus, these equations are not thermodynamically consistent with the subsequently developed IAPWS equations of state for fluid and solid H<sub>2</sub>O. The newer equations of state are "The IAPWS Formulation 1995 for the Thermodynamic Properties of Ordinary Water Substance for General and Scientific Use"<sup>2,3</sup> (called IAPWS-95 for short) and "The Equation of State of H<sub>2</sub>O Ice Ih."<sup>4,5</sup>

In order to make the equations for the sublimation and melting pressures consistent with the IAPWS-95 formulation and the ice Ih equation of state, new correlation equations for the sublimation pressure and melting pressure of ice Ih were developed. In addition, the melting-pressure equation of ice III was slightly modified to make it consistent with the

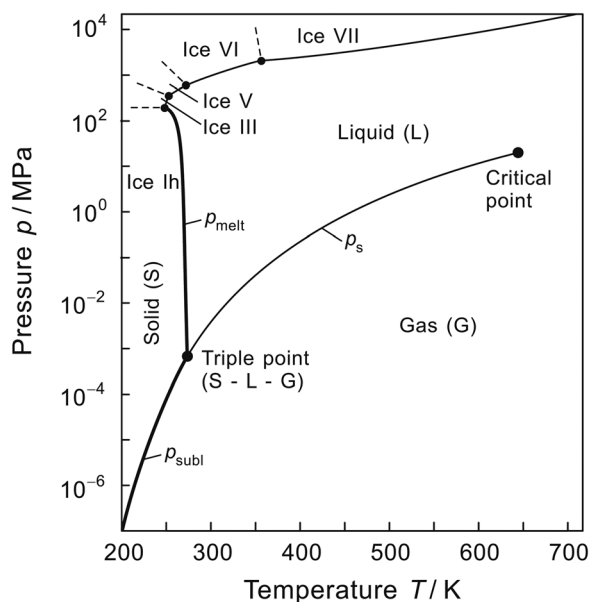


Fig. 1. Phase-boundary curves of water in a  $p$ - $T$  diagram. For a reasonable pressure scale in this figure, the sublimation-pressure curve  $p_{\text{subl}}$  was truncated at 200 K.

melting-pressure equation of ice Ih at the ice Ih–ice III–liquid triple point; see Fig. 1. Although the IAPWS melting-pressure equations for ice V, ice VI, and ice VII are unchanged, they are included in this article for completeness. All of these equations are also given in the corresponding IAPWS Release.<sup>6</sup>

Since the (normal) vapor–liquid–solid triple point, where the solid, liquid, and gas phases of water are in equilibrium (see Fig. 1), is of importance for the topics considered in this work, its temperature and pressure values are given here. The temperature is defined in the International Temperature Scale of 1990 (ITS-90)<sup>7</sup> to be

$$T_t = 273.16 \text{ K.} \quad (1a)$$

Based on the widely accepted measurements of Guildner *et al.*,<sup>8</sup> the triple-point pressure is

$$p_t = (611.657 \pm 0.010) \text{ Pa.} \quad (1b)$$

The relative uncertainty of the triple-point pressure amounts to 0.0016%. These uncertainties correspond to an expanded uncertainty at the  $k=3$  level (three times the standard uncertainty).

Both the IAPWS-95 formulation<sup>2,3</sup> and the equation of state for ice Ih<sup>4,5</sup> yield for the triple-point pressure the value,

$$p_t = 611.654771 \text{ Pa.} \quad (1c)$$

The difference between the pressure values given by Eqs. (1b) and (1c) is extremely small and well within the experimental uncertainty.

## 2. Input Data for the Development of the New Equations

The input data for the new equations for the sublimation pressure and the melting pressure for ice Ih were determined by applying the phase-equilibrium condition between the two phases in thermodynamic equilibrium along the sublimation-pressure curve and the melting-pressure curve, respectively.

### 2.1. Input data for the sublimation-pressure equation

The input data for the development of the sublimation-pressure equation were determined from the phase-equilibrium condition at the sublimation-pressure curve, namely

$$g^+(T, p) = g''(T, p), \quad (2)$$

where  $g^+$  is the specific Gibbs energy of ice Ih at the sublimation-pressure curve and  $g''$  is the specific Gibbs energy of gaseous water (water vapor) at the sublimation-pressure curve. The quantity  $g^+$  is calculated from the equation of state for ice Ih,<sup>4,5</sup> and  $g''$  is calculated from the IAPWS-95 formulation.<sup>2,3</sup> For given values of temperature, the corresponding sublimation pressure,  $p_{\text{subl}}$ , was determined from Eq. (2) by iteration; the iteration tolerance for equality of specific Gibbs energy was set to  $10^{-8} \text{ kJ kg}^{-1}$ . In this way, values for the sublimation pressure were calculated from the temperature of the triple point,  $T_t = 273.16 \text{ K}$ , down to 130 K. This is the lowest temperature for which the specific Gibbs energy can be calculated from IAPWS-95, because the range of validity of the equation for the isobaric heat capacity in the ideal-gas state, used in IAPWS-95, extends down only to 130 K.<sup>2</sup>

Table 1 lists some examples for the sublimation-pressure input data obtained from the procedure described above for the temperature range from 273 K down to 130 K. These data also illustrate the magnitudes of the sublimation pressures over this range. The complete set of input data used for the development of the sublimation-pressure equation contained about 250 points. The temperature and pressure values at the triple point were not included in the input data, but were taken into account by a constraint (see Sec. 3).

TABLE 1. Selected input data points on the sublimation curve calculated via the phase-equilibrium condition, Eq. (2), using the IAPWS-95 formulation<sup>2</sup> for water vapor and the equation of state for ice Ih.<sup>4</sup>

$T/\text{K}$	$p_{\text{subl}}/\text{Pa}$	$T/\text{K}$	$p_{\text{subl}}/\text{Pa}$
273	$6.036\,717\,87 \times 10^2$	200	$1.625\,953\,24 \times 10^{-1}$
272	$5.557\,230\,06 \times 10^2$	180	$5.392\,122\,10 \times 10^{-3}$
270	$4.700\,764\,77 \times 10^2$	160	$7.728\,901\,37 \times 10^{-5}$
265	$3.059\,209\,33 \times 10^2$	150	$6.095\,677\,59 \times 10^{-6}$
260	$1.958\,076\,01 \times 10^2$	140	$3.366\,204\,44 \times 10^{-7}$
250	$7.601\,672\,20 \times 10^1$	130	$1.200\,376\,34 \times 10^{-8}$
230	$8.947\,945\,33 \times 10^0$		

The input data for the temperature range from 125 K down to 30 K were taken from Table 4 in the article of Feistel and Wagner.<sup>9</sup> There, the sublimation pressures were also determined by evaluating the phase-equilibrium condition, where  $g^+$  was again calculated from the equation of state for ice Ih,<sup>4,5</sup> but  $g''$  was calculated from the equation of state for the ideal gas in connection with the ideal-gas isobaric heat capacities derived by Woolley<sup>10</sup> at multiples of 10 K. The use of the equation of state for the ideal gas introduces no significant uncertainty for the input data in this range, because at these extremely small pressures there is practically no difference between the thermodynamic properties of “real” water vapor and of water vapor considered as an ideal gas. [After this work was completed, an extension of the ideal-gas part of IAPWS-95 was developed for temperatures from 50 K to 130 K.<sup>11,12</sup> Thus, the input data for the sublimation pressure at lower temperatures could be calculated in the same way as was done for the range from 130 K to 273.16 K. However, tests have shown that data calculated in that manner would be negligibly different from the input data used here.]

## 2.2. Input data for the melting-pressure equation for ice Ih

The input data for the development of the melting-pressure equation for ice Ih were determined from the phase-equilibrium condition at the melting-pressure curve, namely

$$g^+(T, p) = g^{++}(T, p), \quad (3)$$

where  $g^+$  is the specific Gibbs energy of ice Ih at the melting-pressure curve and  $g^{++}$  is the specific Gibbs energy of liquid water at the melting-pressure curve. The quantity  $g^+$  is calculated from the equation of state for ice Ih<sup>4,5</sup> and  $g^{++}$  is calculated from the IAPWS-95 formulation.<sup>2,3</sup> The evaluation of Eq. (3) was carried out by a procedure analogous to that described in Sec. 2.1 for determining the input data for the sublimation-pressure equation. The input data for the melting-pressure equation were calculated from the temperature of the vapor–liquid–solid triple point,  $T_t = 273.16$  K, down to 251.165 K, the temperature of the ice Ih–ice III–liquid triple point.

Table 2 lists some examples for the melting-pressure input data obtained from the procedure described above for the temperature range from 273 K down to 251 K. These data

TABLE 2. Selected input data points on the melting-pressure curve calculated via the phase-equilibrium condition, Eq. (3), using the IAPWS-95 formulation<sup>2</sup> for liquid water and the equation of state for ice Ih.<sup>4</sup>

$T/K$	$p_{\text{melt}}/\text{MPa}$	$T/K$	$p_{\text{melt}}/\text{MPa}$
273	$2.145\,341\,88 \times 10^0$	260	$1.382\,698\,77 \times 10^2$
272	$1.513\,552\,02 \times 10^1$	255	$1.794\,134\,79 \times 10^2$
270	$3.931\,333\,88 \times 10^1$	253	$1.948\,406\,74 \times 10^2$
265	$9.233\,519\,36 \times 10^1$	251	$2.097\,797\,49 \times 10^2$

also illustrate the magnitudes of the melting pressures over this range. The complete set of input data used for the development of the melting-pressure equation contained more than 200 points. The temperature and pressure values at the triple point were not included in the input data, but were taken into account by the structure of the melting-pressure equation (see Sec. 4).

## 3. The New Sublimation-Pressure Equation

The previous IAPWS sublimation-pressure equation<sup>1</sup> contained two terms and was developed based on the experimental data of Douslin and Osborn<sup>13</sup> and Jancso *et al.*<sup>14</sup> Because the lowest temperature of these data was 194 K, this sublimation-pressure equation was only valid from the triple-point temperature of 273.16 K down to 190 K.

The new sublimation-pressure equation was developed based on two steps that have proved to be successful for establishing empirical equations for the calculation of thermodynamic properties.<sup>2,15,16</sup> These steps are the formulation of a convenient “bank of terms” and the application of the structure-optimization method of Setzmann and Wagner<sup>17</sup> to determine from the bank of terms the best combination of a selected number of terms. After several tests, a structure for the new equation was finally selected that is similar to the structure of reference-quality vapor-pressure equations, e.g., for water<sup>2</sup> and sulfur hexafluoride.<sup>15</sup> In these optimization steps, the respective equations were fitted to the sublimation-pressure input data set described in Sec. 2.1. This procedure resulted in the following equation for the sublimation pressure of water:

$$\ln \pi = \theta^{-1} \sum_{i=1}^3 a_i \theta^{b_i}, \quad (4)$$

where  $\pi = p_{\text{subl}}/p^*$  and  $\theta = T/T^*$  with  $T^* = T_t = 273.16$  K and  $p^* = p_t = 611.657$  Pa;  $T_t$  and  $p_t$  are the temperature and pressure values at the triple point. The coefficients  $a_i$  and exponents  $b_i$  are given in Table 3.

Equation (4) exactly reproduces the temperature and pressure of the triple point, Eqs. (1a) and (1b); this was achieved by taking into account the constraint,

$$\sum_{i=1}^3 a_i = 0 \quad (4a)$$

TABLE 3. Coefficients  $a_i$  and exponents  $b_i$  of the sublimation-pressure equation, Eq. (4).

$i$	$a_i$	$b_i$
1	$-0.212\,144\,006 \times 10^2$	$0.333\,333\,333 \times 10^{-2}$
2	$0.273\,203\,819 \times 10^2$	$0.120\,666\,667 \times 10^1$
3	$-0.610\,598\,130 \times 10^1$	$0.170\,333\,333 \times 10^1$

in the optimization process of Eq. (4). The reason for constraining Eq. (4) at the triple-point pressure according to Eq. (1b) and not Eq. (1c) was to remain consistent with the internationally accepted value. Although the input data used extended down to 30 K (see Sec. 2.1), the lower limit for the range of validity of Eq. (4) was chosen as 50 K in order to avoid an additional term that would have been needed to extend the range by only 20 K. Moreover, sublimation pressures at such low temperatures have little practical relevance because of their extremely low values; at 50 K, the sublimation pressure is about  $1.9 \times 10^{-40}$  Pa.

*Computer-program verification:* To assist the user in computer-program verification of Eq. (4), the following value is given:  $T = 230.0$  K,  $p = 8.947$  35 Pa.

### 3.1. Discussion of the sublimation-pressure equation

Figure 2 compares the sublimation-pressure values calculated from Eq. (4) (zero line) with the input data used for the development of this equation. For temperatures from 130 K up to 273.16 K, corresponding to the range where the input data calculated from the phase-equilibrium condition exist (see Table 1), the upper diagram illustrates that Eq. (4) represents these data to within 0.005% above and within 0.02% below 250 K. This is negligible in comparison to the uncertainty of the input data; see Sec. 3.2. The deviations of values calculated from the more complex seven-term equation of Feistel and Wagner<sup>9</sup> are shown for comparison. The lower

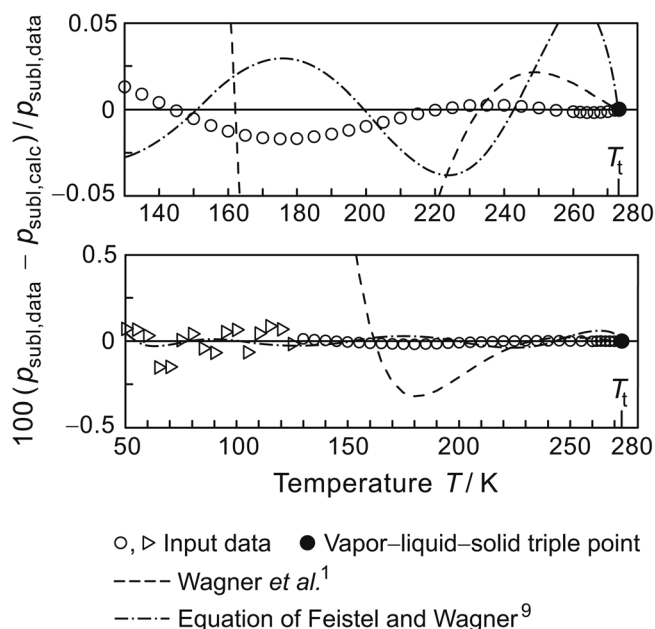


FIG. 2. Percentage deviations in sublimation pressure between the input data  $p_{\text{subl,data}}$  (examples are given in Table 1) and the values  $p_{\text{subl,calc}}$  calculated with Eq. (4). The lower diagram (with a different deviation scale) covers the entire range of validity of Eq. (4) and shows the position of the input data for the range between 50 and 125 K. Values from the equation of Feistel and Wagner<sup>9</sup> and the previous IAPWS sublimation-pressure equation<sup>1</sup> are shown for comparison.

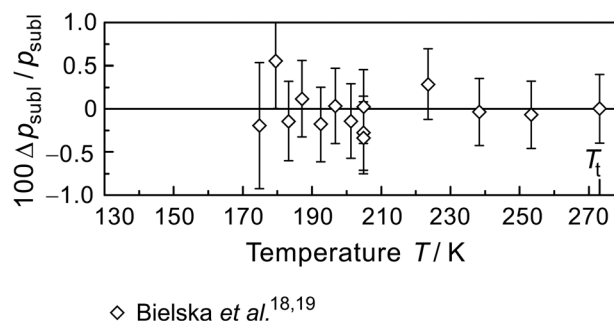


FIG. 3. Percentage deviations  $[100 \Delta p_{\text{subl}} / p_{\text{subl}} = 100(p_{\text{subl,exp}} - p_{\text{subl,calc}}) / p_{\text{subl,exp}}]$  of experimental data for the sublimation pressure  $p_{\text{subl,exp}}$  from values  $p_{\text{subl,calc}}$  calculated with Eq. (4). The error bars depict standard uncertainties ( $k = 1$ ) of the experimental data.

diagram illustrates that Eq. (4) also represents the input data for the range between 50 K and 130 K to within the scatter of the data. It can be seen that the previous IAPWS sublimation-pressure equation<sup>1</sup> deviates significantly from all of the data and from Eq. (4).

Figure 3 shows the deviations of experimental sublimation pressures measured very recently by Bielska *et al.*<sup>18,19</sup> from the values calculated with Eq. (4). The differences are well within the uncertainties of the data given by the authors; except for four data points, the agreement is within 0.2%. These experimental data were not available at the time the new sublimation-pressure equation was developed. Considering this, it is notable how well Eq. (4) agrees with these new measurements<sup>18,19</sup> (or vice versa). When taking into account the expanded uncertainty ( $k = 2$ ) of Eq. (4) (see Sec. 3.2) and the uncertainties of the experimental data (the error bars shown in Fig. 3 only correspond to the standard uncertainty  $k = 1$ ), it can be concluded that the sublimation pressures of H<sub>2</sub>O can (at the present time) be more accurately calculated than measured.

A comparison of sublimation-pressure data measured between 1965 and 2011<sup>13,14,18–22</sup> (only Weber's data<sup>23</sup> are much older) with the values from Eq. (4) is presented in Fig. 4. These data cover a temperature range from 132 to 273.16 K. The upper diagram with a deviation scale of  $\pm 20\%$  shows that there are significant differences among the data of the various authors but also considerable scatter within the data of the same author. The differences between the data of Mauersberger and Krankowsky<sup>20</sup> and the values from Eq. (4) extend to about  $-35\%$  at about 165 K, and the data of Bryson *et al.*<sup>22</sup> deviate from the equation values by more than 150% at about 132 K (not shown in the figure). The lower diagram shows the data situation using a deviation scale of  $\pm 1\%$  (data with deviations greater than 1% were omitted). For temperatures from 255 to 273.16 K, the experimental sublimation pressures of Douslin and Osborn<sup>13</sup> and Jancso *et al.*<sup>14</sup> lie about  $\pm 0.2\%$  around the zero line, while the measurements of Bielska *et al.*<sup>18,19</sup> completely agree with the values from Eq. (4); see also Fig. 3. These new measurements significantly improve the situation of the experimental sublimation pressures.

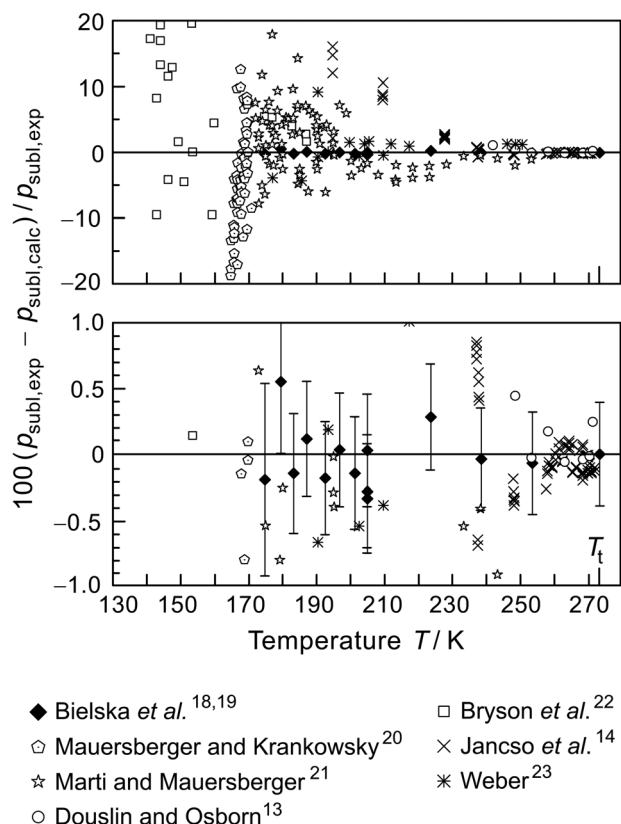


Fig. 4. Percentage deviations of experimental data for the sublimation pressure  $p_{\text{subl,exp}}$  from values  $p_{\text{subl,calc}}$  calculated with Eq. (4). Data with deviations outside the two different deviation scales were omitted. The error bars given for the experimental data of Bielska *et al.*<sup>18,19</sup> depict standard uncertainties ( $k = 1$ ).

### 3.2. Range of validity and estimated uncertainty of the sublimation-pressure equation

The range of validity of the sublimation-pressure equation, Eq. (4), covers the sublimation-pressure curve in the temperature range from 50 to 273.16 K. It fully meets the triple point according to Eq. (1b).

The expanded uncertainty in sublimation pressure according to Eq. (4) was estimated from the equations derived in the Appendix. For temperatures above 130 K, it is

$$\left[ \frac{U(p_{\text{subl}})}{p_{\text{subl}}} \right]^2 \approx (1.1 \times 10^{-5})^2 + \left[ 1 \times 10^{-2} \left( \frac{T_t}{T} - 1 \right) \right]^2 + \left[ 4 \times 10^{-4} \left( \frac{T_t}{T} - 1 - \ln \frac{T_t}{T} \right) \right]^2 \quad (5a)$$

and between 50 K and 130 K the equation reads

$$\left[ \frac{U(p_{\text{subl}})}{p_{\text{subl}}} \right]^2 \approx (1.1 \times 10^{-5})^2 + \left[ 1 \times 10^{-2} \left( \frac{T_t}{T} - 1 \right) \right]^2 + \left[ 1.4 \times 10^{-4} + 0.4 \times 10^{-1} \times \left( \frac{130 \text{ K}}{T} - 1 - \ln \frac{130 \text{ K}}{T} \right) \right]^2. \quad (5b)$$

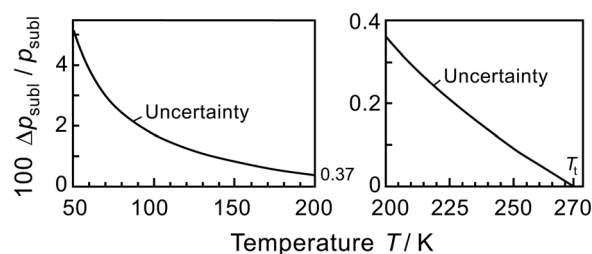


Fig. 5. Percentage uncertainties in sublimation pressure for the sublimation-pressure equation, Eq. (4), estimated with Eqs. (5a) and (5b). The uncertainties correspond to expanded uncertainties with a coverage factor  $k = 2$ . The estimate for the uncertainty at the triple-point temperature is 0.0011%.

Figure 5 is the graphical illustration of the uncertainties from Eqs. (5a) and (5b).

## 4. The New Melting-Pressure Equation for Ice Ih

The previous IAPWS melting-pressure equation<sup>1</sup> for ice Ih contains two terms and was determined based on the experimental data of Bridgman<sup>24</sup> and of Henderson and Speedy.<sup>25</sup>

The new melting-pressure equation was developed based on a procedure very similar to that used for the determination of the new sublimation-pressure equation, Eq. (4). Several tests showed that the basic mathematical form used for the terms of the previous equation was also most effective for the new melting-pressure equation. Based on this result, the structure-optimization method of Setzmann and Wagner<sup>17</sup> was again applied to determine the final equation. In these optimization steps, the respective equations were fitted to the melting-pressure input data set described in Sec. 2.2. This procedure resulted in the following equation for the melting pressure of H<sub>2</sub>O ice Ih:

$$\pi = 1 + \sum_{i=1}^3 a_i (1 - \theta^{b_i}), \quad (6)$$

where  $\pi = p_{\text{melt}}/p^*$  and  $\theta = T/T^*$  with  $T^* = T_t = 273.16$  K and  $p^* = p_t = 611.657$  Pa;  $T_t$  and  $p_t$  are the temperature and pressure values at the vapor–liquid–solid triple point. The coefficients  $a_i$  and exponents  $b_i$  are listed in Table 4.

As a consequence of its structure, for  $T = 273.16$  K Eq. (6) yields exactly the pressure at the triple point according to Eq. (1b). The reason for selecting for the reducing pressure  $p^*$  the triple-point pressure  $p_t$  according to Eq. (1b) and not

TABLE 4. Coefficients  $a_i$  and exponents  $b_i$  of the melting-pressure equation, Eq. (6).

$i$	$a_i$	$b_i$
1	$0.119\,539\,337 \times 10^7$	$0.300\,000 \times 10^1$
2	$0.808\,183\,159 \times 10^5$	$0.257\,500 \times 10^2$
3	$0.333\,826\,860 \times 10^4$	$0.103\,750 \times 10^3$

Eq. (1c) was to remain consistent with the internationally accepted value.

*Computer-program verification:* To assist the user in computer-program verification of Eq. (6), the following value is given:  $T = 260.0$  K,  $p = 138.268$  MPa.

#### 4.1. Discussion, range of validity, and estimated uncertainty of the melting-pressure equation for ice Ih

Figure 6 compares the melting-pressure values calculated from Eq. (6) (zero line) with the input data used for the development of this equation. These input data were calculated from the phase-equilibrium condition ice Ih–liquid (see Sec. 2.2) and cover the temperature range from 251.165 K up to 273.16 K (i.e., the range between the ice Ih–ice III–liquid triple point and the vapor–liquid–solid triple point); see Table 2. The upper diagram illustrates that Eq. (6) represents these data to within  $\pm 0.002\%$  over the entire range of the melting-pressure curve for ice Ih. This small difference in pressure corresponds to about 0.5 mK in temperature (on average over the entire melting-pressure curve). These differences are negligible in comparison to the uncertainty of the input data, which produce the uncertainty of Eq. (6) as discussed below. From the lower diagram with a different

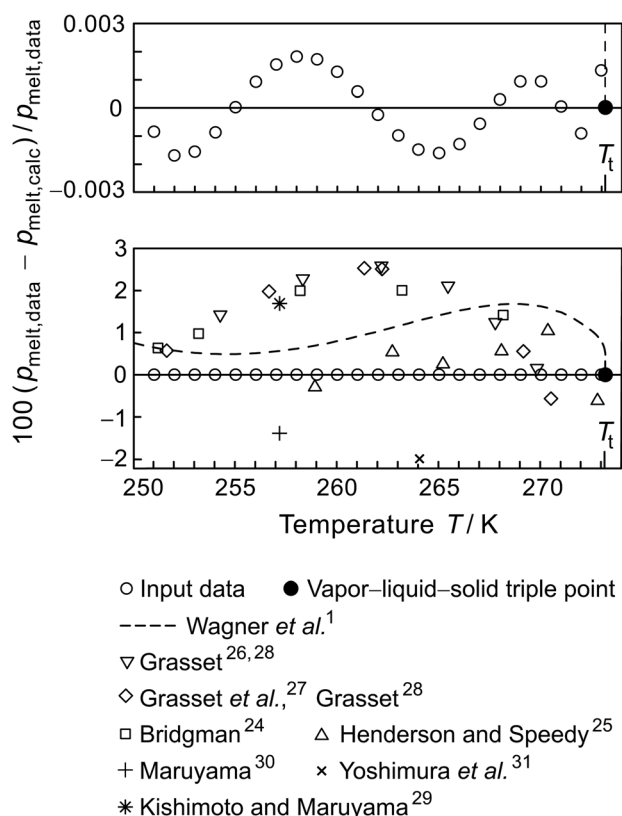


FIG. 6. Percentage deviations in melting pressure between the input data  $p_{\text{melt,data}}$  (examples are given in Table 2) and the values  $p_{\text{melt,calc}}$  calculated with Eq. (6). For comparison, the lower diagram (with a different deviation scale) also shows the deviations of values calculated from the previous IAPWS melting-pressure equation<sup>1</sup> and of experimental data.

deviation scale, it can be seen that the previous IAPWS melting-pressure equation<sup>1</sup> deviates significantly from Eq. (6). The same applies to the experimental melting pressures of Bridgman<sup>24</sup> and of Henderson and Speedy,<sup>25</sup> which were used for the development of the previous equation. More recent experimental melting pressures are given in graphical form in the articles of Grasset<sup>26</sup> and Grasset *et al.*<sup>27</sup> The numerical values of these data were provided by Grasset.<sup>28</sup> In addition to these sources, there are three papers<sup>29–31</sup> that contain one melting-pressure data point each, which are also plotted in Fig. 6. As discussed for the sublimation-pressure equation, the uncertainty of Eq. (6) is clearly smaller than the uncertainty of the experimental data. On the other hand, all these experimental data agree with the values from Eq. (6) within their experimental uncertainty.

*Range of validity:* Equation (6) is valid for the entire melting-pressure curve of ice Ih, i.e., from 251.165 K to 273.16 K, from the ice Ih–ice III–liquid triple point to the vapor–liquid–solid triple point.

*Estimate of uncertainty:* The expanded uncertainty ( $k = 2$ ) of the melting-pressure equation for ice Ih is estimated to be 2% in pressure.<sup>4</sup> This is a conservative estimate that was carried out similarly to the estimation of the uncertainty for the sublimation-pressure equation, Eq. (4).

## 5. Melting-Pressure Equations for Ice III, Ice V, Ice VI, and Ice VII

Although the IAPWS melting-pressure equations for ice V, ice VI, and ice VII are unchanged compared to the Release of 1993 and the corresponding paper,<sup>1</sup> they are included in this article for completeness. The IAPWS melting-pressure equation for ice III was slightly adjusted to agree with the ice Ih melting-pressure equation at the corresponding triple point.

### 5.1. Melting-pressure equation for ice III

Compared to the previous IAPWS melting-pressure equation of ice III,<sup>1</sup> the coefficient and the pressure  $p^*$  were slightly modified to make Eq. (7) consistent with the melting-pressure equation of ice Ih, Eq. (6), at the ice Ih–ice III–liquid triple point; see Fig. 1. The adjusted melting-pressure equation for ice III is

$$\pi = 1 - 0.299948(1 - \theta^{60}), \quad (7)$$

where  $\pi = p_{\text{melt}}/p^*$  and  $\theta = T/T^*$  with  $T^* = 251.165$  K and  $p^* = 208.566$  MPa. The values for  $T^*$  and  $p^*$  correspond to the temperature and pressure at the ice Ih–ice III–liquid triple point, respectively, as shown in Table 5. The range of validity of Eq. (7) covers temperatures from 251.165 K to 256.164 K. For the uncertainty and the values for computer-program verification of Eq. (7), see Tables 6 and 7. Based on the relatively high uncertainties of the experimental melting pressures, the derivatives of Eq. (7) could be subject to larger relative errors.

TABLE 5. Values for the triple points of the solid phases that coexist with another solid phase and with the liquid.

Coexisting phases	$T_i/K$	$p_i/MPa$
ice Ih – ice III – liquid	251.165	208.566 <sup>a</sup>
ice III – ice V – liquid	256.164	350.1
ice V – ice VI – liquid	273.31	632.4
ice VI – ice VII – liquid	355	2216

<sup>a</sup> This is not the experimental triple-point pressure  $p_{t,exp}$ , but was calculated to make, at this triple point, Eqs. (6) and (7) consistent with each other. The difference ( $p_{t,exp} - p_{t,calc}$ ) is 0.64% of the triple-point pressure, which is clearly within the 3% uncertainty of the experimentally determined triple-point pressure.<sup>24</sup>

## 5.2. Melting-pressure equations for ice V, ice VI, and ice VII

The IAPWS melting-pressure equations for these modifications of ice are unchanged compared to the Release of 1993 and the corresponding paper;<sup>1</sup> they are included in this article for completeness.

**Melting pressure of ice V (temperature range from 256.164 K to 273.31 K):**

$$\pi = 1 - 1.18721(1 - \theta^8), \quad (8)$$

where  $\pi = p_{melt}/p^*$  and  $\theta = T/T^*$  with  $T^* = 256.164$  K and  $p^* = 350.1$  MPa.

**Melting pressure of ice VI (temperature range from 273.31 K to 355 K):**

$$\pi = 1 - 1.07476(1 - \theta^{4.6}), \quad (9)$$

where  $\pi = p_{melt}/p^*$  and  $\theta = T/T^*$  with  $T^* = 273.31$  K and  $p^* = 632.4$  MPa.

**Melting pressure of ice VII (temperature range from 355 K to 715 K):**

$$\begin{aligned} \ln \pi = & 0.173683 \times 10^1 (1 - \theta^{-1}) \\ & - 0.544606 \times 10^{-1} (1 - \theta^5) \\ & + 0.806106 \times 10^{-7} (1 - \theta^{22}), \end{aligned} \quad (10)$$

where  $\pi = p_{melt}/p^*$  and  $\theta = T/T^*$  with  $T^* = 355$  K and  $p^* = 2216$  MPa.

**Note:** The upper value of the temperature range of Eq. (10) corresponds to the highest temperature for which measurements exist and not the end of the melting curve of ice VII.

TABLE 6. Estimated uncertainties of the calculated melting pressures.

Equation	Equilibrium	Uncertainty
(7)	ice III – liquid	3%
(8)	ice V – liquid	3%
(9)	ice VI – liquid	3%
(10)	ice VII – liquid	7%

TABLE 7. Melting pressures calculated from Eqs. (7) to (10) for selected temperatures.

Equation	Equilibrium	$T/K$	$p/MPa$
(7)	ice III – liquid	254.0	268.685
(8)	ice V – liquid	265.0	479.640
(9)	ice VI – liquid	320.0	1356.76
(10)	ice VII – liquid	550.0	6308.71

Equations (8) to (10) are constrained to fit the experimental temperature and pressure values of the relevant triple points given in Table 5.

### 5.2.1. Range of validity and estimates of uncertainty of the equations

Equations (8) and (9) are valid for the entire range of the solid-liquid equilibrium for the ice form stated. Equation (10) only covers the range of the solid-liquid equilibrium for ice VII up to 715 K, as indicated.

The estimated uncertainties of the melting pressures calculated from Eqs. (8) to (10) are listed in Table 6. Based on the relatively high uncertainties of the experimental melting pressures, the derivatives of Eqs. (8) to (10) could be subject to larger errors.

### 5.2.2. Computer-program verification

To assist the user in computer-program verification, Table 7 lists values for the pressures calculated from each of the equations at one temperature within its range of validity.

## 6. Acknowledgments

The authors thank the members of the IAPWS Working Group “Thermophysical Properties of Water and Steam” for fruitful discussions. In addition, we thank J. T. Hodges for making the data from Ref. 19 available prior to publication. Our thanks also go to K. Mauersberger for providing the data from Refs. 20 and 21 and to O. Grasset for providing the data from Refs. 26 and 27.

## 7. Appendix: Uncertainty Estimate for the Sublimation-Pressure Equation

In the sublimation range of  $T$  and  $p$ , the specific Gibbs energy of water vapor can be estimated with sufficient accuracy by

$$\begin{aligned} g^{\text{vap}}(T, p) = & g_0 + s_0 T + RT \ln p + pB(T) \\ & + \int_{T_i}^T \left(1 - \frac{T}{T'}\right) \cdot c_p^{\text{id}}(T') dT', \end{aligned} \quad (A1)$$

where  $B(T)$  is the second virial coefficient, which may be estimated from IAPWS-95<sup>2,3</sup> or from the correlation of Harvey and Lemmon.<sup>32</sup> The specific Gibbs energy of ice Ih can be estimated by



$$g^{\text{Ih}}(T, p) = g^{\text{Ih}}(T, p_t) + v^{\text{Ih}}(T, p_t)(p - p_t). \quad (\text{A2})$$

The constants  $g_0$  and  $s_0$  can be expressed by the vapor–liquid–solid triple-point properties. From equating the specific Gibbs energies of ice Ih and water vapor, the expression for the sublimation pressure,  $p_{\text{subl}}(T)$ , is obtained,

$$\begin{aligned} RT \ln p_{\text{subl}} + p_{\text{subl}} [B(T) - v^{\text{Ih}}(T, p_t)] \\ = RT \ln p_t + p_t \left[ B(T_t) - v^{\text{Ih}}(T, p_t) + (T - T_t) \left( \frac{dB(T)}{dT} \right)_{T=T_t} \right] \\ + (T - T_t) s^{\text{vap}}(T_t, p_t) \\ - \int_{T_t}^T \left[ \left( 1 - \frac{T}{T'} \right) \cdot c_p^{\text{id}}(T') + s^{\text{Ih}}(T', p_t) \right] dT'. \quad (\text{A3}) \end{aligned}$$

We consider possible deviations  $\delta$  of the various quantities from their true values, and the way these deviations are correlated by Eq. (A3), at a given exact temperature  $T$ , exactly defined triple-point temperature  $T_t$ , and  $R$  considered as exact,

$$\begin{aligned} \frac{\delta p_{\text{subl}}}{p_{\text{subl}}} = \frac{\delta p_t}{p_t} + \frac{p_{\text{subl}} - p_t}{RT} \delta v^{\text{Ih}}(T, p_t) + \left[ \frac{p_t}{T_t} - \frac{p_{\text{subl}}}{T} \right] \frac{\delta B(T_t)}{R} \\ - \left( \frac{1}{T} - \frac{1}{T_t} \right) \frac{p_t \delta \left[ T_t \left( \frac{dB(T)}{dT} \right)_{T=T_t} - B(T_t) \right]}{R} \\ + \frac{p_{\text{subl}}}{RT} \delta [B(T_t) - B(T)] + \left( 1 - \frac{T_t}{T} \right) \frac{\delta s^{\text{vap}}(T_t, p_t)}{R} \\ - \int_{T_t}^T \left( \frac{1}{T} - \frac{1}{T'} \right) \frac{\delta c_p^{\text{id}}(T')}{R} dT' + \frac{1}{T} \int_{T_t}^T \frac{\delta s^{\text{Ih}}(T', p_t)}{R} dT'. \quad (\text{A4}) \end{aligned}$$

Some minor terms compared to the ideal-gas volume were neglected here. We now consider the individual deviations of Eq. (A4) as statistically independent and infer for their related expanded ( $k=2$ ) uncertainties  $U$  the equation,

$$\begin{aligned} \left[ \frac{U(p_{\text{subl}})}{p_{\text{subl}}} \right]^2 = \left[ \frac{U(p_t)}{p_t} \right]^2 + \left[ \frac{(p_t - p_{\text{subl}}) U(v^{\text{Ih}}(T, p_t))}{RT} \right]^2 + \left[ \left( \frac{p_t}{T_t} - \frac{p_{\text{subl}}}{T} \right) \frac{U(B(T_t))}{R} \right]^2 \\ + \left[ \left( \frac{1}{T} - \frac{1}{T_t} \right) \frac{p_t U \left( B(T_t) - T_t \left( \frac{dB(T)}{dT} \right)_{T=T_t} \right)}{R} \right]^2 + \left[ \frac{p_{\text{subl}} U(B(T_t) - B(T))}{RT} \right]^2 \\ + \left[ \left( \frac{T_t}{T} - 1 \right) \frac{U(s^{\text{vap}}(T_t, p_t))}{R} \right]^2 + \left[ \int_{T_t}^T \left( \frac{1}{T} - \frac{1}{T'} \right) \frac{U(c_p^{\text{id}}(T'))}{R} dT' \right]^2 + \left[ \frac{1}{T} \int_{T_t}^T \frac{U(s^{\text{Ih}}(T', p_t))}{R} dT' \right]^2. \quad (\text{A5}) \end{aligned}$$

Reasonable estimates for the various quantities involved here show that only four of them are practically relevant.

- (1) The experimental uncertainty of the triple-point pressure was estimated by Guildner *et al.*,<sup>8</sup> with the value of 0.010 Pa as an expanded uncertainty at the  $k=3$  level; see Eq. (1b). For a  $k=2$  expanded uncertainty, we multiply the value of 0.010 Pa by 2/3,

$$\frac{U(p_t)}{p_t} = \frac{2}{3} \times \frac{0.01}{611.657} \approx 1.1 \times 10^{-5}. \quad (\text{A6})$$

The dominant contributions below the triple point result from the uncertainties of the entropies of vapor and of ice, points (2), (3), and (4) below.

- (2) To estimate the vapor-entropy term of Eq. (A5),

$$\left( \frac{T_t}{T} - 1 \right) \frac{U(s^{\text{vap}}(T_t, p_t))}{R}, \quad (\text{A7})$$

we use the IAPWS-95 uncertainty of the vapor entropy at the triple point (Ref. 4, p. 1036, and Ref. 9, p. 43, and Fig. 4 of the IAPWS Advisory Note No. 1<sup>33</sup>),

$$\frac{U(s^{\text{vap}}(T_t, p_t))}{s^{\text{vap}}(T_t, p_t)} = 2 \times 10^{-4}. \quad (\text{A8})$$

With the value of the triple-point entropy of vapor,

$$s^{\text{vap}}(T_t, p_t) \approx 9000 \text{ J kg}^{-1} \text{ K}^{-1}, \quad (\text{A9})$$

we obtain the estimate,

$$\begin{aligned} \left( \frac{T_t}{T} - 1 \right) \frac{U(s^{\text{vap}}(T_t, p_t))}{R} \\ \approx \left( \frac{T_t}{T} - 1 \right) \frac{1.8}{462} \approx 4 \times 10^{-3} \left( \frac{T_t}{T} - 1 \right). \quad (\text{A10}) \end{aligned}$$

- (3) The ideal-gas term of Eq. (A5),

$$-\int_{T_i}^T \left(\frac{1}{T} - \frac{1}{T'}\right) \frac{U(c_p^{\text{id}}(T'))}{R} dT' \quad (\text{A11})$$

can be estimated using the uncertainty of the isobaric heat capacity of water vapor above 130 K,  $U(c_p)/c_p \approx 0.01\%$ ,

$$\frac{U(c_p^{\text{id}}(T'))}{c_p^{\text{id}}(T')} = 1 \times 10^{-4}, \quad (\text{A12})$$

with the result

$$\begin{aligned} & -\int_{T_i}^T \left(\frac{1}{T} - \frac{1}{T'}\right) \frac{U(c_p^{\text{id}}(T'))}{R} dT' \\ & \approx -\frac{1 \times 10^{-4}}{462 \text{ J kg}^{-1} \text{ K}^{-1}} \int_{T_i}^T \left(\frac{1}{T} - \frac{1}{T'}\right) c_p^{\text{id}}(T') dT'. \end{aligned} \quad (\text{A13})$$

Down to 50 K, the isobaric heat capacity of vapor is sufficiently well approximated by

$$c_p^{\text{id}} \approx 2000 \text{ J kg}^{-1} \text{ K}^{-1}. \quad (\text{A14})$$

We carry out the integral in Eq. (A13),

$$\begin{aligned} & -\int_{T_i}^T \left(\frac{1}{T} - \frac{1}{T'}\right) \frac{U(c_p^{\text{id}}(T'))}{R} dT' \\ & \approx 0.4 \times 10^{-3} \left(\frac{T_i}{T} - 1 - \ln \frac{T_i}{T}\right). \end{aligned} \quad (\text{A15})$$

At 130 K, this uncertainty is

$$0.4 \times 10^{-3} \left(\frac{T_i}{130 \text{ K}} - 1 - \ln \frac{T_i}{130 \text{ K}}\right) \approx 1.4 \times 10^{-4}. \quad (\text{A16})$$

Below 130 K, the correlation for the sublimation pressure is based on linear interpolation between the Woolley<sup>10</sup> grid points carried out in Ref. 9, Fig. 3. Very likely, the interpolation leads to an error larger than the uncertainties of Woolley's data. For simplicity, we conservatively infer from Fig. 3 of Ref. 9 that the interpolation error of  $c_p^{\text{id}}$  does not exceed 1% between 130 K and 50 K. With this value, we get for  $T < 130$  K,

$$\begin{aligned} & -\int_{T_i}^T \left(\frac{1}{T} - \frac{1}{T'}\right) \frac{U(c_p^{\text{id}}(T'))}{R} dT' \\ & \approx 1.4 \times 10^{-4} + 0.4 \times 10^{-1} \left(\frac{130 \text{ K}}{T} - 1 - \ln \frac{130 \text{ K}}{T}\right). \end{aligned} \quad (\text{A17})$$

(4) For the final term of Eq. (A5),

$$-\frac{1}{T} \int_{T_i}^T \frac{U(s^{\text{lh}}(T', p_i))}{R} dT', \quad (\text{A18})$$

we use the uncertainty estimate for the ice entropy ( $k=2$ ),<sup>9</sup>

$$U(s^{\text{lh}}(T, p_i)) = 4 \text{ J kg}^{-1} \text{ K}^{-1}, \quad (\text{A19})$$

and calculate the integral,

$$-\frac{1}{T} \frac{4}{462} \int_{T_i}^T dT' \approx 9 \times 10^{-3} \left(\frac{T_i}{T} - 1\right). \quad (\text{A20})$$

**Result:** Summing up the contributions (1)–(4), our final result for Eq. (A5) reads above 130 K,

$$\begin{aligned} \left[\frac{U(p_{\text{subl}})}{p_{\text{subl}}}\right]^2 & \approx (1.1 \times 10^{-5})^2 + \left[1 \times 10^{-2} \left(\frac{T_i}{T} - 1\right)\right]^2 \\ & + \left[4 \times 10^{-4} \left(\frac{T_i}{T} - 1 - \ln \frac{T_i}{T}\right)\right]^2, \end{aligned} \quad (\text{A21a})$$

and between 50 K and 130 K,

$$\begin{aligned} \left[\frac{U(p_{\text{subl}})}{p_{\text{subl}}}\right]^2 & \approx (1.1 \times 10^{-5})^2 + \left[1 \times 10^{-2} \left(\frac{T_i}{T} - 1\right)\right]^2 \\ & + \left[1.4 \times 10^{-4} + 0.4 \times 10^{-1}\right. \\ & \left. \times \left(\frac{130 \text{ K}}{T} - 1 - \ln \frac{130 \text{ K}}{T}\right)\right]^2. \end{aligned} \quad (\text{A21b})$$

Equations (A21a) and (A21b) correspond to Eqs. (5a) and (5b), respectively.

## 8. References

- <sup>1</sup>W. Wagner, A. Saul, and A. Pruß, *J. Phys. Chem. Ref. Data* **23**, 515 (1994).
- <sup>2</sup>W. Wagner and A. Pruß, *J. Phys. Chem. Ref. Data* **31**, 387 (2002).
- <sup>3</sup>IAPWS, *Revised Release on the IAPWS Formulation 1995 for the Thermodynamic Properties of Ordinary Water Substance for General and Scientific Use* (2009). Available from <http://www.iapws.org>.
- <sup>4</sup>R. Feistel and W. Wagner, *J. Phys. Chem. Ref. Data* **35**, 1021 (2006).
- <sup>5</sup>IAPWS, *Revised Release on the Equation of State 2006 for H<sub>2</sub>O Ice Ih* (2009). Available from <http://www.iapws.org>.
- <sup>6</sup>IAPWS, *Revised Release on the Pressure along the Melting and Sublimation Curves of Ordinary Water Substance* (2011). Available from <http://www.iapws.org>.
- <sup>7</sup>H. Preston-Thomas, *Metrologia* **27**, 3 (1990).
- <sup>8</sup>L. A. Guildner, D. P. Johnson, and F. E. Jones, *J. Res. Natl. Bur. Stand.* **80A**, 505 (1976).
- <sup>9</sup>R. Feistel and W. Wagner, *Geochim. Cosmochim. Acta* **71**, 36 (2007).
- <sup>10</sup>H. W. Woolley, "Thermodynamic Properties for H<sub>2</sub>O in the Ideal Gas State," in *Water and Steam – Their Properties and Current Industrial Applications, Proceedings of the 9th International Conference on the Properties of Steam*, edited by J. Straub and K. Scheffler (Pergamon Press, Oxford, 1980), p. 166.
- <sup>11</sup>R. Feistel, D. G. Wright, H.-J. Kretzschmar, E. Hagen, S. Herrmann, and R. Span, *Ocean Sci.* **6**, 91 (2010).
- <sup>12</sup>IOC, SCOR, IAPSO, *The International Thermodynamic Equation of Seawater – 2010: Calculation and Use of Thermodynamic Properties*, Intergovernmental Oceanographic Commission, Manuals and Guides No. 56 (UNESCO, Paris, 2010). Available at <http://www.TEOS-10.org>.
- <sup>13</sup>R. Douslin and A. Osborn, *J. Sci. Instrum.* **42**, 369 (1965).

- <sup>14</sup>G. Jancso, J. Pupezin, and W. van Hook, *J. Phys. Chem.* **74**, 2984 (1970).
- <sup>15</sup>C. Guder and W. Wagner, *J. Phys. Chem. Ref. Data* **38**, 33 (2009).
- <sup>16</sup>D. Bücker and W. Wagner, *J. Phys. Chem. Ref. Data* **35**, 205 (2006).
- <sup>17</sup>U. Setzmann and W. Wagner, *Int. J. Thermophys.* **10**, 1103 (1989).
- <sup>18</sup>K. Bielska, D. K. Havey, G. E. Scace, D. Lisak, and J. T. Hodges, *Proc. Royal Soc. A* (in press).
- <sup>19</sup>K. Bielska, D. K. Havey, D. Lisak, G. E. Scace, A. H. Harvey, R. D. van Zee, and J. T. Hodges, *J. Geophys. Res.* (unpublished).
- <sup>20</sup>K. Mauersberger and D. Krankowsky, *Geophys. Res. Lett.* **30**, 1121 (2003).
- <sup>21</sup>J. Marti and K. Mauersberger, *Geophys. Res. Lett.* **20**, 363 (1993).
- <sup>22</sup>C. E. Bryson III, V. Cazcarra, and L. L. Levenson, *J. Chem. Eng. Data* **19**, 107 (1974).
- <sup>23</sup>S. Weber, *Commun. Phys. Lab. Univ. Leiden* **150**, (1915). [The data are reproduced in H. Spencer-Gregory and E. Rourke, *Hygrometry* (Crosby Lockwood and Son, London, 1957)].
- <sup>24</sup>P. W. Bridgman, *Proc. Am. Acad. Arts Sci.* **47**, 441 (1912).
- <sup>25</sup>S. J. Henderson and R. J. Speedy, *J. Phys. Chem.* **91**, 3069 (1987).
- <sup>26</sup>O. Grasset, *High Press. Res.* **21**, 139 (2001).
- <sup>27</sup>O. Grasset, E. Amiguet, and M. Choukroun, *High Press. Res.* **25**, 155 (2005).
- <sup>28</sup>O. Grasset (private communication).
- <sup>29</sup>Y. Kishimoto and M. Maruyama, *Rev. High Pressure Sci. Technol.* **7**, 1144 (1998).
- <sup>30</sup>M. Maruyama, *J. Cryst. Growth* **275**, 598 (2005).
- <sup>31</sup>Y. Yoshimura, H.-K. Mao, and R. J. Hemley, *J. Phys.: Conf. Ser.* **121**, 042004 (2008).
- <sup>32</sup>A. H. Harvey and E. W. Lemmon, *J. Phys. Chem. Ref. Data* **33**, 369 (2004).
- <sup>33</sup>IAPWS, Advisory Note No. 1: *Uncertainties in Enthalpy for the IAPWS Formulation 1995 for the Thermodynamic Properties of Ordinary Water Substance for General and Scientific Use (IAPWS-95) and the IAPWS Industrial Formulation 1997 for the Thermodynamic Properties of Water and Steam (IAPWS-IF97)* (2003). Available from <http://www.iapws.org>.